

Quantum Chemical Calculation of the Catalytic Reaction of Ethane Dehydrogenation on Gallium Oxide–Hydroxide Binuclear Clusters in Oxidized GaO/ZSM-5 Zeolite

I. V. Kuz'min^a, G. M. Zhidomirov^{a,b}, V. N. Solkan^a, and V. B. Kazanskii^a

^a Zelinskii Institute of Organic Chemistry, Russian Academy of Sciences, Moscow, 119991 Russia

^b Boreskov Institute of Catalysis, Siberian Branch, Russian Academy of Sciences, Novosibirsk, 630090 Russia

e-mail: solkanvn@ioc.ac.ru

Received September 3, 2008

Abstract—The catalytic activity of oxidized GaO/HZSM-5 in the reaction of alkane dehydrogenation can be due to hydrogenated gallium oxide clusters stabilized in the cationic positions of the zeolite. The binuclear gallium oxide clusters $[\text{Ga}_2\text{O}_2]^{2+}$ in oxidized gallium-substituted high-silica zeolite HZSM-5, which are isomeric to two gallyl ions $[\text{GaO}]^+$ stabilized on two spatially separated lattice aluminum ions, were considered using the DFT method within the framework of a cluster approach. It was found that, even in the case of a relatively large distance between these aluminum ions, gallium oxide particles in oxidized GaO/HZSM-5 can occur as charged planar $[\text{Ga}_2\text{O}_2]^{2+}$ four-membered rings. These cluster particles exhibited a high affinity to hydrogen, and they were readily hydrogenated with the retention of their structural integrity. It was demonstrated that this partially hydrogenated cluster could be responsible for the catalytic process of ethane dehydrogenation. In the first step, ethane dissociatively added to the $[\text{Ga}_2\text{O}_2\text{H}_2]^{2+}$ cluster. Then, the ethylene molecule was eliminated from the resulting intermediate to leave the $[\text{Ga}_2\text{O}_2\text{H}_4]^{2+}$ cluster. The cycle was closed by the elimination of a hydrogen molecule with the formation of the initial structure of $[\text{Ga}_2\text{O}_2\text{H}_2]^{2+}$.

DOI: 10.1134/S0023158409050188

INTRODUCTION

Gallium-containing zeolites ZSM-5 are efficient catalysts for the dehydrogenation of light alkanes to alkenes followed by aromatization [1]. On this basis, the commercial Cyclar process was implemented [2]. However, in spite of great efforts made by researchers, the structure of the active centers of these catalysts remains open to question. In this context, the oxidized form of GaO/HZSM-5 catalysts is the most ambiguous. Interest in this problem is also stimulated by the facts that, as found previously, the introduction of O_2 into a reaction mixture resulted in an increase in the rate of reaction [3] and the oxidized GaO/HZSM-5 samples exhibited a noticeably higher rate of reaction than reduced ones [4]. Initially, the structure of gallyl ions $[\text{GaO}]^+$ that might appear at first glance to be obvious was proposed as an oxidized gallium species stabilized in zeolite [5]. These cations consist of a gallium atom with a formal charge of +3, which is partially neutralized by an oxygen atom with a formal charge of -2 to give the resulting charge of +1, which is compensated by a negatively charged aluminum tetrahedron of zeolite. It was hypothesized that $[\text{GaO}]^+$ cations exhibit high catalytic activity in the reaction of ethane dehydrogenation [6, 7]. The mechanism of this

reaction on zeolites was studied previously with the use of computation methods [8, 9].

Since then, the structure of gallyl ions $[\text{GaO}]^+$ has been widely used to interpret experimental results [10–12] and to perform theoretical calculations [9, 13, 14]. Both the high activity of this structure, for example, in the heterolytic dissociation of light alkanes, and serious problems in the regeneration of this structure in the course of closing a catalytic cycle were noted in theoretical studies [9, 14]. In particular, for this reason, it was concluded that the $[\text{GaO}]^+$ species cannot be a catalytic site for the reaction of ethane dehydrogenation [15]. The high chemical activity of gallyl cations implies their instability and possible evolution into other species, for example, by dimerization with the formation of binuclear gallium oxide clusters.

In the majority of publications, the possibility of formation of polynuclear gallium clusters in zeolites was only mentioned for a long time. However, this idea began to develop in recent years. For example, Rozanska et al. [16] reported a theoretical study of the formation of binuclear gallium hydride clusters in mordenite. Hensen et al. [17] discussed the stability of binuclear gallium hydride–hydroxide clusters. They calculated that these clusters can be formed by the dimerization of neighboring $[\text{HGaOH}]^+$ cations and Ga^+ upon the treatment of gallium-substituted HZSM-5 with water. They also noted that these clus-

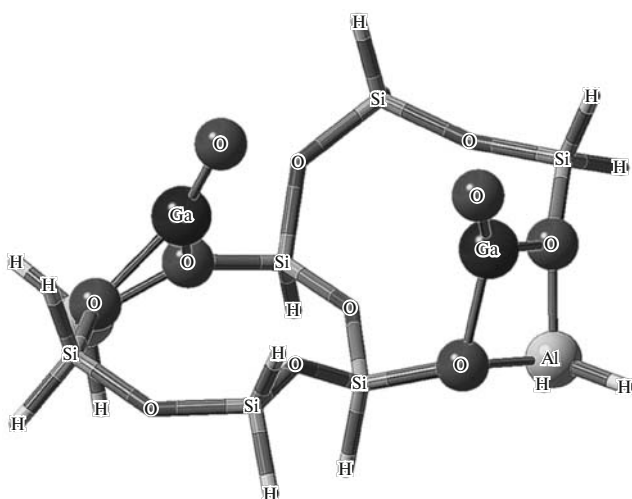


Fig. 1. Optimized structure of the active center with two separated GaO^+ cationic fragments arranged at different aluminum tetrahedrons in zeolite.

ters can exhibit activity in alkane dehydrogenation. Zhidomirov et al. [18] noted that there is a clearly pronounced tendency to the formation of $[\text{Ga}_2\text{O}_2]^{2+}$ binuclear oxide particles from two $[\text{GaO}]^+$ cations in the case of their occurrence in a zeolite ring. The previously found [17, 18] structures of binuclear clusters exhibited a common feature: gallium and oxygen atoms formed a Ga_2O_2 four-membered ring with alternating atoms, which can be considered as two condensed GaO particles.

In this work, we consider an analogous complex with two $[\text{GaO}]^+$ cations, but with a longer distance between charge-compensating lattice aluminum atoms (>7 Å) arranged at conjugated five-membered zeolite rings. We calculated the reaction mechanism of ethane dehydrogenation on the proposed binuclear cluster structure and demonstrated that the reaction of C–H bond cleavage and the recombination removal of hydrogen occurred on the partially hydrogenated form of this cluster with appropriate energy barriers.

INVESTIGATION TECHNIQUES

In this study, the crystal lattice of zeolite ZSM-5 was simulated with a cluster built from two rings each containing five silicon atoms and conjugated via oxygen and two silicon atoms bound to it. The accurate positions of silicon and oxygen atoms were taken from the structure of ZSM-5 (MFI orthorhombic lattice) found by X-ray diffraction [19]. One silicon atom in each of the zeolite rings was replaced by aluminum atoms (Fig. 1). Hydrogen atoms were added to silicon and aluminum atoms; these hydrogen atoms were oriented along the external Si–O and Al–O dangling bonds at initially specified distances of 1.47 and 1.58 Å, respectively, which were subsequently opti-

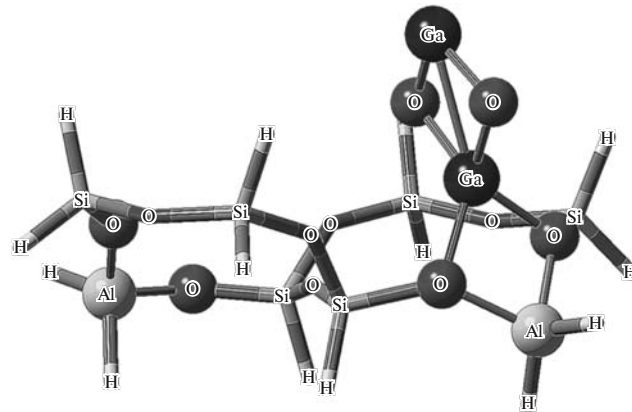


Fig. 2. Optimized structure of the four-membered cyclic cluster Ga_2O_2 oriented perpendicularly to the AlO_2 plane of zeolite lattice.

mized. Four model structures with the general formula Ga_2O_2 were arranged onto this framework: two separated $[\text{GaO}]^+$ ions, planar four-membered rings formed by alternating gallium and oxygen atoms, and a linear peroxide cluster as a chain formed so that gallium atoms were joined through two oxygen atoms ($\text{Ga}–\text{O}–\text{O}–\text{Ga}$). The structures were arranged on the zeolite framework so that gallium atoms were oriented to the oxygens of aluminum tetrahedrons.

Quantum chemical calculations were performed by the density functional theory (DFT) using the GAUSSIAN 03 program [20] with TCP Linda. The hybrid B3LYP functional [21–23] was used; the D95 basis set was used for hydrogen, silicon, and aluminum atoms, whereas the 6-31G* basis set was chosen for gallium, oxygen, and carbon.

The geometric parameters of the structures were optimized in two steps. At the first step, the framework was frozen and only the Si–H and Al–H distances between the terminal hydrogen atoms and framework silicon and aluminum atoms were optimized. The resulting coordinates of hydrogen atoms were used for the subsequent calculations. At the next step, the Cartesian coordinates of hydrogen atoms were frozen and all of the other atoms were set free. In the optimization of hydrogenated cluster structures and their derivatives, the coordinates of framework atoms in the zeolite lattice were fixed in addition to terminal hydrogen atoms. The transition states of elementary reactions were found using the QST2 and QST3 algorithms [24, 25] in the frozen framework with testing the reactants and products along the reaction coordinate.

RESULTS AND DISCUSSIONS

The gallium oxide cluster structures with a formal charge of +2 were formed by the association of two $[\text{GaO}]^+$ ions (Figs. 1–3). The charge was compensated by two lattice aluminum atoms arranged at a distance

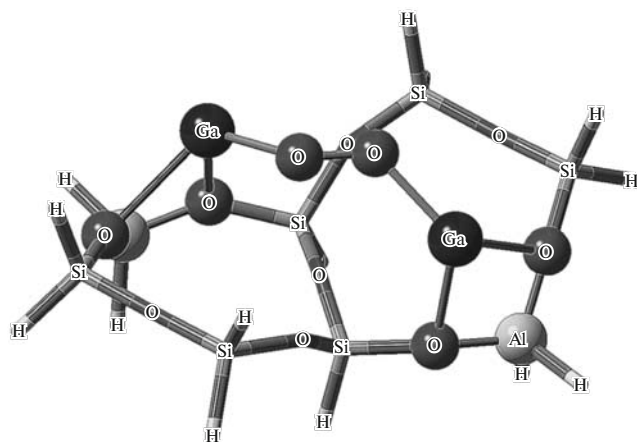


Fig. 3. Structure of the unstable peroxide chain Ga_2O_2 obtained after the first step of optimization.

of 7.2–7.5 Å from each other, which were put in place of silicon atoms in a zeolite cluster of eight tetrahedrons. The cationic cluster structures were arranged as a planar quasi-square four-membered ring with alternating Ga and O atoms (Fig. 2) and as a $[\text{GaOOGa}]^{2+}$ chain cluster (Fig. 3) of the peroxide type. For comparison, a structure with two separated $[\text{GaO}]^+$ cations at corresponding cationic positions was calculated as a model (Fig. 1).

As a result of the geometry optimization, considerable structure rearrangements did not occur only in the structure containing two $[\text{Ga}=\text{O}]^+$ oxo ions (Fig. 1). Although the chain structure retained its shape after the first step of optimization (Fig. 3), they deformed after the second step so that both of the oxygen atoms were above a gallium atom to form the cationic pair of $[\text{GaO}_2]^+$ and Ga^+ (Fig. 4). The distance between these oxygen atoms was 1.58 Å, which is almost 0.4 Å longer than that in molecular oxygen (Table 1). The square-planar $[\text{Ga}_2\text{O}_2]^{2+}$ was elevated over the framework and oriented perpendicularly to its

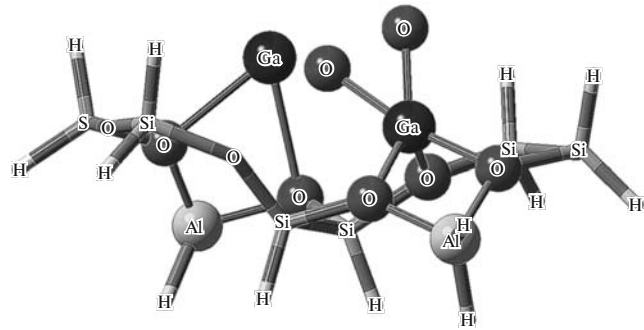


Fig. 4. Optimized structure with Ga^+ and GaO_2^+ cations obtained after the subsequent optimization of the gallium peroxide chain (Fig. 3).

plane (Fig. 2); in this case, one of the Ga atoms moved away from the position over the oxygens of aluminum so that the entire $[\text{Ga}_2\text{O}_2]^{2+}$ structure was over only one of the aluminum atoms. The localization of the $[\text{Ga}_2\text{O}_2]^{2+}$ ring was either coplanar (Fig. 5) or perpendicular (Fig. 2) to the AlO_2 plane. Geometrically, the planar four-membered Ga_2O_2 ring (Figs. 2, 5) was an almost perfect square with an insignificant deformation due to a small shift of the external Ga atom to the center of the square.

A minimum Ga–O distance of 1.68 Å (Table 1) and a maximum distance of 4.69 Å between gallium atoms were found in the structure shown in Fig. 1.

The lowest energy was found for the structure with separated $[\text{GaO}]^+$ fragments (Table 2). In this case, the energy of the coplanar form of the adsorbed square cluster was higher by only 0.1 kcal/mol. The energies of the other isomeric structures were only slightly higher than the above values. Thus, the energies of the perpendicularly oriented square cluster and the structure with both oxygen atoms at one gallium atom were higher than the energy of the first structure by 3.9 and 5.1 kcal/mol, respectively. However, the difference in energies was not so great to unambiguously suggest the

Table 1. Optimized bond lengths and interatomic distances (in Å) for the proposed cluster structures, as compared with the traditional representation of two gallyl ions

	Two separated $\text{Ga}=\text{O}$ fragments	Ga_2O_2 ring (perpendicularly oriented)	Ga_2O_2 ring (coplanar)	Ga^+ and GaO_2^+
Ga–Ga	4.96	2.53	2.59	3.89
O–O	4.32	2.73	2.73	1.58
Ga(1)–O(1)	1.68	1.82	2.00	1.84
Ga(1)–O(2)	5.22	1.83	1.95	1.94
Ga(2)–O(1)	4.56	1.90	1.79	3.31
Ga(2)–O(2)	1.68	1.90	1.79	2.24
Ga(1)–Al(1)	2.88	7.34	3.00	3.00
Ga(2)–Al(2)	2.80	2.78	6.28	3.38

predominance of the first form. It is more likely that the simultaneous coexistence of various oxidized gallium forms, including small oxide clusters, adsorbed on zeolite channel walls can be assumed.

Our previous calculations [26] demonstrated that the gallyl ions $[\text{GaO}]^+$ readily move around an aluminum tetrahedron with an activation energy of 18.6 kcal/mol. The high mobility of these ions on a support can result in the orientation of two $[\text{GaO}]^+$ dipole fragments toward one another; in turn, this orientation will facilitate the trapping of one gallyl by the other to form a condensed oxide particle of $[\text{Ga}_2\text{O}_2]^{2+}$. Another mechanism of the formation of a square Ga_2O_2 particle in the oxidation of gallium-substituted zeolite can also be proposed. At the first step, gallium is oxidized to form a $[\text{GaO}_2]^+$ particle (Fig. 4), which can result from the adsorption of molecular oxygen by gallium or the consecutive oxidation by two equivalents of N_2O [27]. Then, the gallium cation migrates to the $[\text{GaO}_2]^+$ particle with the formation of the resulting square cluster.

Next, we considered the binuclear cyclic cluster $[\text{Ga}_2\text{O}_2]^{2+}$ as an active catalytic site in alkane dehydrogenation reactions. Before the simulation of the overall mechanism of a catalytic reaction, we studied the interaction of this cluster with molecular hydrogen because it is believed that the activation of the recombination removal of hydrogen is the main function of gallium in gallium–zeolite catalysts [1]. The hydrogen molecule can be added to the cluster in a number of manners to obtain a set of dihydrides (Fig. 6) with different energies of formation (dissociative adsorption of hydrogen), which are summarized in Table 3. Evidently, this process is strongly exothermic except for

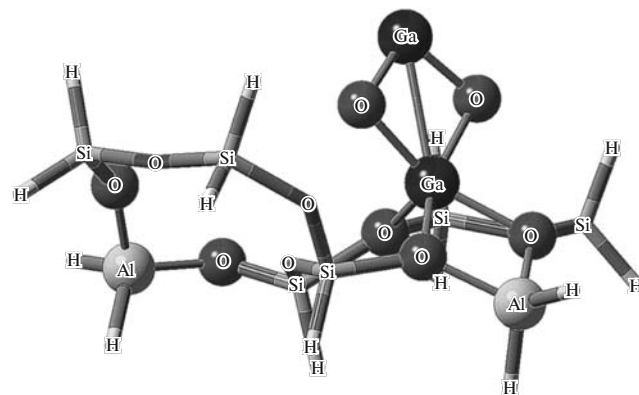


Fig. 5. Optimized structure of the four-membered cyclic cluster $[\text{Ga}_2\text{O}_2]^{2+}$ coplanar to the AlO_2 plane of zeolite lattice.

the case of structure II (Fig. 6). For example, the energy of adsorption for channel I is $\Delta E = -77.1$ kcal/mol (Table 3). The activation energy of this process is only 12.6 kcal/mol, whereas the activation energy of hydrogen desorption from resulting dihydride I is 89.7 kcal/mol (Table 4). On this basis, we can conclude that the adsorption of the first H_2 molecule on $[\text{Ga}_2\text{O}_2]^{2+}$ occurs readily and almost irreversibly. Hence, it follows that the $[\text{Ga}_2\text{O}_2\text{H}_2]^{2+}$ cluster cannot efficiently release H_2 after the completion of an ethane dehydrogenation cycle and the desorption of an ethylene molecule in the case of the simulation of this reaction on the $[\text{Ga}_2\text{O}_2]^{2+}$ center. Next, we consider the formation of a tetrahydride cluster (Fig. 7a). The second hydrogen molecule is analogously arranged on a cluster: one of the hydrogen atoms added to the free

Table 2. Relative energies (in kcal/mol) of various $[\text{Ga}_2\text{O}_2]^{2+}$ cluster structures, as compared with separated GaO^+ cations

	Two separated $\text{Ga}=\text{O}$ fragments	Ga_2O_2 ring (perpendicularly oriented)	Ga_2O_2 ring (coplanar)	Ga^+ and GaO_2^+
$[\text{Ga}=\text{O}]^+ + [\text{Ga}=\text{O}]^+$	—	-3.9	-0.1	-5.1
Ga_2O_2 ring (perpendicular)	3.9	—	3.8	-1.2
Ga_2O_2 ring (coplanar)	0.1	-3.8	—	-5.0
$\text{Ga}^+ + [\text{GaO}_2]^+$	5.1	1.2	5.0	—

Table 3. Relative electronic energies (ΔE) of the proposed cluster dihydrides and the tetrahydride, as compared with the initial $[\text{Ga}_2\text{O}_2]^{2+}$ cluster with consideration for the energies of hydrogen molecules

Structure	ΔE , kcal/mol
Dihydride (Fig. 6, I)	-77.1
Dihydride (Fig. 6, II)	30.0
Dihydride (Fig. 6, III)	-68.3
Dihydride (Fig. 6, IV)	-92.9
Tetrahydride (Fig. 7a)	-96.6

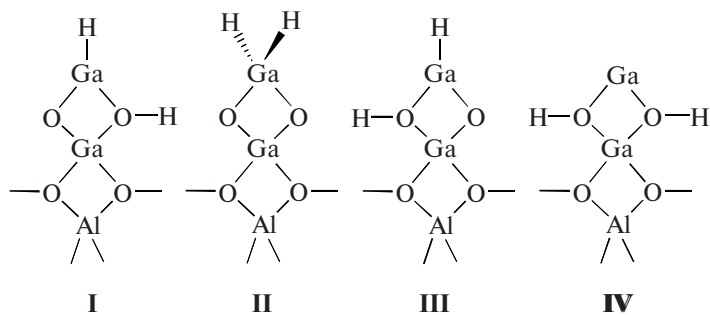
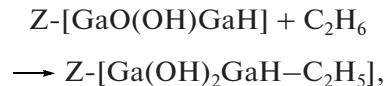


Fig. 6. Isomeric $[\text{Ga}_2\text{O}_2\text{H}_2]^{2+}$ dihydrides obtained upon the adsorption of a hydrogen molecule onto the four-membered ring $[\text{Ga}_2\text{O}_2]^{2+}$.

bridging oxygen atom, and the other, to the terminal GaH group to form the symmetrical tetrahydride $[\text{Ga}(\text{OH})_2\text{GaH}_2]^{2+}$. This reaction is also exothermic but not as strongly as the addition of the first hydrogen molecule, and the energy of the system changed by -19.5 kcal/mol (Table 3). The reaction has a relatively low activation barrier (23.8 kcal/mol), which resulted in an activation energy of 43.3 kcal/mol for the elimination of a hydrogen molecule from the tetrahydride (Table 4). Thus, we conclude that the removal of H_2 from $[\text{Ga}_2\text{O}_2\text{H}_4]^{2+}$ is possible, and we can consider the reaction mechanism of ethane dehydrogenation on the hydrogenated cluster $[\text{Ga}_2\text{O}_2\text{H}_2]^{2+}$ rather than on $[\text{Ga}_2\text{O}_2]^{2+}$ (Table 5).

We found the structure of the dissociative adsorption of an ethane molecule on the hydrogenated cluster. In this case, the ethyl fragment was bound to the external gallium atom, whereas hydrogen was bound to the bridging oxygen atom (Fig. 7b). This structure resulted from the reaction



which occurred with an energy gain of -9.1 kcal/mol and an activation energy of 32.8 kcal/mol (Table 5). Next, we considered the elimination of the ethylene molecule

Table 4. Energies (ΔE) and electronic activation barriers (E_a) of the consecutive hydrogenation reactions of the cyclic cluster $[\text{Ga}_2\text{O}_2]^{2+}$ (with the specified geometry parameters of transition states)

Reaction	$[\text{Ga}_2\text{O}_2]^{2+} + \text{H}_2 \longrightarrow [\text{Ga}_2\text{O}_2\text{H}_2]^{2+}$	$[\text{Ga}_2\text{O}_2\text{H}_2]^{2+} + \text{H}_2 \longrightarrow [\text{Ga}_2\text{O}_2\text{H}_4]^{2+}$
Ga–H distance in TS, Å	1.91	1.85
O–H distance in TS, Å	1.49	1.34
H–H distance in TS, Å	0.91	0.99
Activation energy of the forward reaction E_a , kcal/mol	12.6	23.8
Activation energy of the reverse reaction E'_a , kcal/mol	89.7	43.3
ΔE , kcal/mol	−77.1	−19.5

Table 5. Energies (ΔE) and electronic activation barriers (E_a) of the reaction of ethane dehydrogenation on the hydrogenated four-membered cluster $[\text{Ga}_2\text{O}_2\text{H}_2]^{2+}$

Reaction	Activation energy of the forward reaction E_a , kcal/mol	Activation energy of the reverse reaction E'_a , kcal/mol	ΔE , kcal/mol
$\text{Z-}[\text{Ga}_2\text{O}_2\text{H}_2] + \text{C}_2\text{H}_6 \longrightarrow \text{Z-}[\text{Ga}_2\text{O}_2\text{H}_3-\text{C}_2\text{H}_5]$	32.8	41.8	−9.1
$\text{Z-}[\text{Ga}_2\text{O}_2\text{H}_3-\text{C}_2\text{H}_5] \longrightarrow \text{Z-}[\text{Ga}_2\text{O}_2\text{H}_4] + \text{C}_2\text{H}_4$	46.5	14.7	31.8

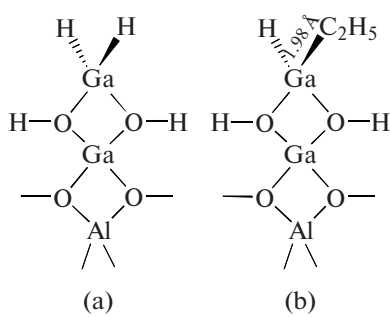
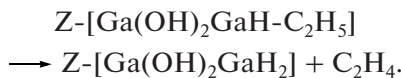


Fig. 7. Derivatives of the cyclic cluster $[\text{Ga}_2\text{O}_2]^{2+}$: (a) tetrahydride and (b) ethane molecule adsorbed on the hydrogenated cluster.



The energy of this process was 46.5 kcal/mol (Table 5), which was lower than or comparable with the results obtained for other active centers (Table 6). Finally, the active center $[\text{Ga}_2\text{O}_2\text{H}_2]^{2+}$ was regenerated from $[\text{Ga}_2\text{O}_2\text{H}_4]^{2+}$ by the removal of a hydrogen molecule, which occurred with a previously found activation energy of 43.3 kcal/mol (Table 4). This allowed us to close the catalytic cycle (Fig. 8).

Evidently, ethane dehydrogenation on the proposed cluster occurs with a lower activation barrier than on Ga^+ and $[\text{GaH}_2]^+$ active centers in reduced samples [6] (Table 6). Joshi and Thomson [28] proposed a reaction mechanism for ethane dehydrogenation on $[\text{GaH}]^{2+}$ particles, which simulate active centers in the reduced state of a gallium–zeolite catalyst and demonstrated that the catalytic activity of this center depends on the distance between aluminum atoms in the zeolite lattice. Table 6 summarizes the energy characteristics of the ethane dehydrogenation reaction on one of these preferable centers [28]. Comparing these data with our results, we can state that the key activation energy on our hydrogenated cluster $[\text{Ga}_2\text{O}_2\text{H}_2]^{2+}$ is close to that found by Joshi and Thom-

son [28]. Thus, based on our data, we can propose the above cluster as a model oxidized catalytic site in the sample of $\text{GaO}/\text{HZSM-5}$ and explain the high rate of catalytic reaction on the oxidized form of gallium-substituted zeolite.

CONCLUSIONS

We hypothesized that the binuclear gallium oxide clusters $[\text{Ga}_2\text{O}_2]^{2+}$ stabilized on an aluminum tetrahedron at a comparatively distant arrangement of the second lattice aluminum ion can serve as active catalytic sites for alkane dehydrogenation reactions in oxidized high-silica zeolites $\text{GaO}/\text{HZSM-5}$. The specified cluster structure is isomeric to two gallyl ions $[\text{GaO}]^+$ stabilized on two spatially separated lattice aluminum ions. We calculated the reaction mechanism of ethane dehydrogenation on this binuclear gallium oxide cluster. We found that molecular hydrogen readily undergoes dissociative adsorption on the gallium oxide cluster to give dihydrides, which can act as active catalytic sites for alkane dehydrogenation reactions. Note that the hydrogen-free gallium oxide cluster cannot be a model of the catalytic site for the catalytic reactions of alkane dehydrogenation because it has a very high affinity to hydrogen and cannot be regenerated by hydrogen removal from the hydride form. However, the situation changes for a partially hydrogenated cluster, for example, for dihydride species. We evaluated the activation energy of the ethane dehydrogenation reaction based on the activation energies of the dissociative adsorption of ethane and the removal of ethylene from the test hydride cluster. We compared the results with published data and concluded that the test reaction can occur on the proposed cluster. It is likely that the formation of such

Table 6. Reaction kinetics of ethane dehydrogenation on various model active centers

Parameter	$\text{Z}^2-[\text{Ga}_2\text{O}_2\text{H}_2]^{2+}$	$\text{Z}^-[\text{GaH}_2]^*$	Z^-Ga^{+*}	$\text{Z}^-[\text{GaH}_2]^{+**}$	$\text{Z}^2-[\text{GaH}]^{2+**}$
Energy of the dissociative adsorption of ethane, kcal/mol	-9.1	8.1	1.14	1.14	10.5
Activation energy of the dissociative adsorption of ethane, kcal/mol	32.8	46.1	52.0	48.6	19.7
Activation energy of the removal of ethylene, kcal/mol	46.5	61.2	53.3	61.7	36.7
Activation energy of the removal of hydrogen, kcal/mol	43.3	46.1	53.3	48.6	47.4
Maximum activation energy, kcal/mol	56.9	69.5	55.7	62.8	62.4

* Data from [6].

** Data from [28].

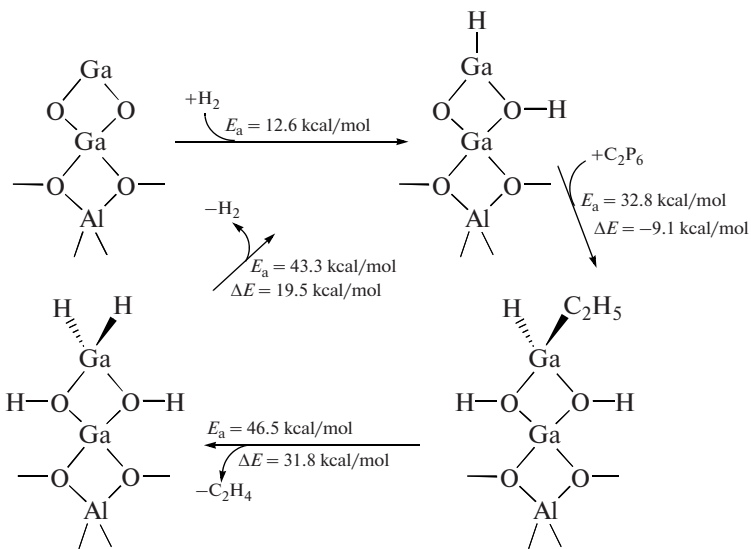


Fig. 8. Catalytic cycle of the mechanism of ethane dehydrogenation on a partially hydrogenated gallium oxide cluster ($[Ga_2O_2H_4]^{2+}$ can be considered as the starting structure, whereas $[Ga_2O_2H_2]^{2+}$ and $[Ga_2O_2H_3C_2H_5]^{2+}$ can be considered as less stable intermediates).

polynuclear gallium oxide–hydroxide structures at the cationic positions of zeolite is responsible for the high activity of oxidized gallium-substituted zeolites ZSM-5 in alkane dehydrogenation reactions.

ACKNOWLEDGMENTS

This work was supported by the Russian Foundation for Basic Research (project no. 05-03-33103).

REFERENCES

1. Biscardi, J.A. and Iglesia, E., *Catal. Today*, 1996, vol. 31, p. 207.
2. Mowry, J.R., Anderson, R.F., and Johnson, J.A., *Oil Gas J.*, 1985, vol. 831, p. 1288.
3. Waku, T., Yu, S.Y., and Iglesia, E., *Ind. Eng. Chem. Res.*, 2003, vol. 42, p. 3680.
4. Hensen, E.J.M., García-Sánchez, M., Rane, N.J., Magusin, P.C.M.M., Liu, P.H., Chao, K.J., and van Santen, R.A., *Catal. Lett.*, 2005, vol. 101, p. 79.
5. El-Malki, El-M., van Santen, R.A., and Sachtler, W.M.H., *J. Phys. Chem. B*, 1999, vol. 103, p. 4611.
6. Pidko, E.A., Kazansky, V.B., Hensen, E.J.M., and van Santen, R.A., *J. Catal.*, 2006, vol. 240, p. 73.
7. Hamid, S.B.A., Derouane, E.G., Meriaudeau, P., and Naccache, C., *Catal. Today*, 1996, vol. 31, p. 327.
8. Kuzmin, I.V., Zhidomirov, G.M., and Hensen, E.J.M., *Catal. Lett.*, 2006, vol. 108, p. 187.
9. Gonzales, N.O., Chakraborty, A.K., and Bell, A.T., *Top. Catal.*, 1999, vol. 9, p. 207.
10. Kazansky, V.B., Subbotina, I.R., van Santen, R.A., and Hensen, E.J.M., *J. Catal.*, 2004, vol. 227, p. 263.
11. Kazansky, V.B., Subbotina, I.R., van Santen, R.A., and Hensen, E.J.M., *J. Catal.*, 2005, vol. 233, p. 351.
12. Rane, N.J., Overweg, A.R., Kazansky, V.B., van Santen, R.A., and Hensen, E.J.M., *J. Catal.*, 2006, vol. 239, p. 478.
13. Broclawik, E., Hime, H., Yamada, M., Kubo, M., Miyamoto, A., and Vetrivel, R., *J. Chem. Phys.*, 1995, vol. 103, p. 2102.
14. Frash, M. and van Santen, R.A., *J. Phys. Chem. A*, 2000, vol. 104, p. 2468.
15. Pidko, E.A., Hensen, E.J.M., and van Santen, R.A., *J. Phys. Chem. C*, 2007, vol. 111, p. 13068.
16. Rozanska, X., García-Sánchez, M., Hensen, E.J.M., and van Santen, R.A., *C. R. Acad. Sci., Ser. IIc: Chim.*, 2005, vol. 8, p. 509.
17. Hensen, E.J.M., Pidko, E.A., Rane, N., and van Santen, R.A., *Angew. Chem., Int. Ed. Engl.*, 2007, vol. 46, p. 7273.
18. Zhidomirov, G.M., Shubin, A.A., Milov, M.A., Hensen, E.J.M., Kazansky, V.B., and van Santen, R.A., *J. Phys. Chem. C*, 2008, vol. 112, p. 3321.
19. Lerner, H., Draeger, M., Steffen, J., and Unger, K.K., *Zeolites*, 1985, vol. 5, p. 131.
20. Frisch, M.J., Trucks, G.W., Schlegel, H.B., Scuseria, G.E., Robb, M.A., Cheeseman, J.R., Montgomery, J.A., Vreven, T., Jr., Kudin, K.N., Burant, J.C., Millam, J.M., Iyengar, S.S., Tomasi, J., Barone, V., Mennucci, B., Cossi, M., Scalmani, G., Rega, N., Petersson, G.A., Nakatsuji, H., Hada, M., Ehara, M., Toyota, K., Fukuda, R., Hasegawa, J., Ishida, M., Nakajima, T., Honda, Y., Kitao, O., Nakai, H., Klene, M., Li, X., Knox, J.E., Hratchian, H.P., Cross, J.B., Adamo, C., Jaramillo, J., Gomperts, R., Stratmann, R.E., Yazyev, O., Austin, A.J., Cammi, R., Pomelli, C., Ochterski, J.W., Ayala, P.Y., Morokuma, K., Voth, G.A., Salvador, P., Dannenberg, J.J., Zakraze-

wski, V.G., Dapprich, S., Daniels, A.D., Strain, M.C., Farkas, O., Malick, D.K., Rabuck, A.D., Raghavachari, K., Foresman, J.B., Ortiz, J.V., Cui, Q., Baboul, A.G., Clifford, S., Cioslowski, J., Stefanov, B.B., Liu, G., Liashenko, A., Piskorz, P., Komaromi, I., Martin, R.L., Fox, D.J., Keith, T., Al-Laham, M.A., Peng, C.Y., Nanayakkara, A., Challacombe, N., Gill, P.M.W., Johnson, B., Chen, W., Wong, M.W., Gonzalez, C., and Pople, J.A., *Gaussian 03, Revision C.02*, Wallingford, Conn.: Gaussian Inc., 2004.

21. Becke, A.D., *Phys. Rev. Sect. A*, 1988, vol. 38, p. 3098.

22. Becke, A.D., *J. Chem. Phys.*, 1993, vol. 98, p. 1372.

23. Becke, A.D., *J. Chem. Phys.*, 1993, vol. 98, p. 5648.

24. Peng, C., Ayala, P.Y., Schlegel, H.B., and Frisch, M.J., *J. Comput. Chem.*, 1996, vol. 17, p. 49.

25. Peng, C. and Schlegel, H.B., *Isr. J. Chem.*, 1993, vol. 33, p. 449.

26. Kusmin, I.V., Zhidomirov, G.M., and Solkan, V.N., *Int. J. Quantum Chem.*, 2007, vol. 107, p. 2434.

27. Solkan, V.N., Zhidomirov, G.M., and Kazansky, V.B., *Int. J. Quantum Chem.*, 2007, vol. 107, p. 2417.

28. Joshi, Y.V. and Thomson, K.T., *Catal. Today*, 2005, vol. 105, p. 106.